Nanoscale

ROYAL SOCIETY OF CHEMISTRY

REVIEW

Cite this: *Nanoscale*, 2020, **12**, 5705

Polyoxometalate-based composite materials in electrochemistry: state-of-the-art progress and future outlook

Dan Wang, Lulu Liu, Jun Jiang, Lijuan Chen* and Junwei Zhao *

Received 13th December 2019,
Accepted 15th February 2020

DOI: 10.1039/c9nr10573e

rsc.li/nanoscale

Polyoxometalates (POMs) have been developed as a class of promising smart material candidates not only due to their multitudinous architectures but also their good redox activities and outstanding electron and proton transport capacities. Recently, abundant studies on POMs composited with metal nanoparticles (NPs), carbon materials (*e.g.*, carbon nanotubes (CNTs), carbon quantum dots (CQDs), graphene), and conducting polymers or highly-porous framework materials (*e.g.*, MOFs, ZIFs) have been performed and POM-based composite materials (PCMs) undoubtedly show enhanced stability and improved electrochemical performances. Therefore, POMs and PCMs are of increasing interest in electrocatalysis, electrochemical detection and energy-related fields (such as fuel cells, redox flow batteries and so on), thus, developing novel PCMs has long been the key research topic in POM chemistry. This review mainly summarizes some representative advances in PCMs with electrochemical applications in the past ten years, expecting to provide some useful guidance for future research.

1. Introduction

With the persistent development of science and technology, an ever-increasing demand for novel smart materials, especially in energy-related fields, has been motivated. Therefore, new materials with excellent electrochemical properties have long been favoured by scientists owing to their extensive applications and great potential in order to meet the demands of cutting-edge technologies. Polyoxometalates (POMs) are a unique class of anionic metal–oxygen clusters constructed from high-valence transition metals (TMs, *e.g.*, V^{V}, Nb^{V}, Ta^{V}, Mo^{VI}, and W^{VI}),[1] and the ammonium salt of $PMo_{12}O_{40}^{3-}$, believed as the first POM, was reported in 1826 by Berzelius.[2] The crystal structure study on POMs is initiated by Keggin with the report on the structure determination of phosphotungstic acid $H_3[PW_{12}O_{40}]\cdot 29H_2O$ according to the powder X-ray diffraction measurement.[3] Another landmark in POM history is the successful realization of isopropyl alcohol production by

Henan Key Laboratory of Polyoxometalate Chemistry, College of Chemistry and Chemical Engineering, Henan University, Kaifeng, Henan 475004, China.
E-mail: ljchen@henu.edu.cn, zhaojunwei@henu.edu.cn

Dan Wang

Dan Wang obtained her BS degree from Henan University in 2012 and then received her PhD in 2018 from the School of Materials Science and Engineering of Shanghai University. Currently, she is working with Prof. Junwei Zhao as a postdoctoral fellow, and her main research interest includes developing functional materials based on rare-earth substituted polyoxometalates with remarkable fluorescence performances as promising candidates in sensing or imaging.

Lulu Liu

Lulu Liu is now studying for her MS degree in Henan University and as a student in the group of Prof. Junwei Zhao at the Henan Key Laboratory of Polyoxometalate Chemistry. Her present research is mainly concentrated on the synthesis of organic–inorganic hybrid rare-earth embedded selenotungstate derivatives and exploration of their electrochemical applications.

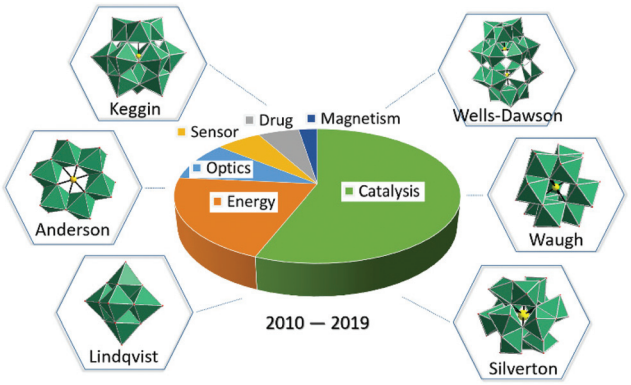

Fig. 1 Classical structure types of POMs and some reported main applications of POM-based materials in recent ten years.

hydration of propylene catalyzed by $H_4SiW_{12}O_{40}$ in Japan in 1972,[4] which attracted the world's explosive attention to POMs. Many novel skeletons of POMs were revealed, thereafter, six classical structures such as Keggin, Anderson, Waugh, Lindqvist, Silverton, and Dawson were consecutively discovered (Fig. 1).[5,6]

Attributing to the high activity of lacunary POM building blocks, hundreds of POM derivatives with more multitudinous and fascinating architectures have been reported through the self-assembly of purely inorganic building blocks (Fig. 2a),[7,8] and/or the bridging functions of metal ions and organic ligands (*e.g.* TM-inserted POMs (Fig. 2b),[4,9,10] rare-earth ions (RE) substituted POMs (Fig. 2c),[11] heterometallic POMs (Fig. 2d),[12,13] and organic ligand modified POMs (Fig. 2e and f)[14–17]). Bearing variable redox activities and outstanding electron and proton transport capacities, POM-based composite materials (PCMs) have displayed some special properties such as the single molecule magnet behavior and optical performances.[11,18,19] Most significantly, POMs have been demonstrated to be powerful electron reservoirs in multi-electron reduction processes,[9,20] which makes them be applied in the electrochemical field.[4,9,21] Another wondrous behavior of PCMs is the proton conductivity, which can entail POMs to be highly proton-conductive materials, and have more new applications such as proton-exchange membrane fuel cells.[22,23] Meanwhile, it has been proved that POMs can function as excellent candidates for the multistep elaboration of PCMs with improved stability and enhanced performances.[42] PCMs provide more ideas for developing neoteric smart materials applied in green catalysis,[43,44] optics,[9] sensors,[45,46] drugs,[6] and energy-related applications[1,47] (Fig. 1). In particular, combining POMs with catalytic nanoparticles (NPs) and/or highly porous materials always contributes to new catalysts with better activity, higher stability and larger specific surface area.[21] In addition, with the help of conducting materials (such as conducting polymers, carbon nanotubes (CNTs) or graphene), PCMs have also been used as electrodes in batteries and supercapacitors.[1,47]

Hitherto, some reviews have been published covering different topics on burgeoning POM sciences. Recently, in 2019, several reviews involving organic–inorganic POMs,[9,15,46] TM-incorporated POMs with biology, catalysis, and magnetism,[43] and POMs as next-generation anticancer metallodrugs,[6] have been already published. Considering the remarkable electrochemical properties of PCMs and booming research achievements, a review on the electrochemical applications of POMs is urgently needed. Therefore, the major advances in the past ten years of PCMs in electrochemistry will be highlighted in this review, which can provide theoretical fundamental and reasonable guidance for future research.

2. Brief summary of PCMs

In the past decade, abundant PCMs have been successively discovered by various preparation methods. This part principally presents a brief summary of some representative PCMs. These PCMs can be divided into four categories according to their different components: (1) POM-based coordination polymers (POMCPs), (2) large organic cation stabilized POM hybrids

Jun Jiang

Jun Jiang obtained her BS degree from the University of Jinan (2009) and MS degree from the College of Chemistry and Molecular Engineering, Zhengzhou University (2012). She is now a PhD candidate at the Henan Key Laboratory of Polyoxometalate Chemistry of Henan University under the supervision of Prof. Junwei Zhao, working on the designed synthesis and the relevant electrochemical and luminescence properties of polyoxometalate-based materials.

Lijuan Chen

Lijuan Chen obtained her BS and MS degrees in chemistry from Henan University (2005) and obtained her PhD under the supervision of Prof. Jianmin Chen at the Lanzhou Institute of Chemical Physics, Chinese Academy of Sciences (2009). At present, she is an Associate Professor at Henan University and her research interest is concentrated on the coordination chemistry of polyoxometalate chemistry and the photophysical properties of polyoxometalate-based materials.

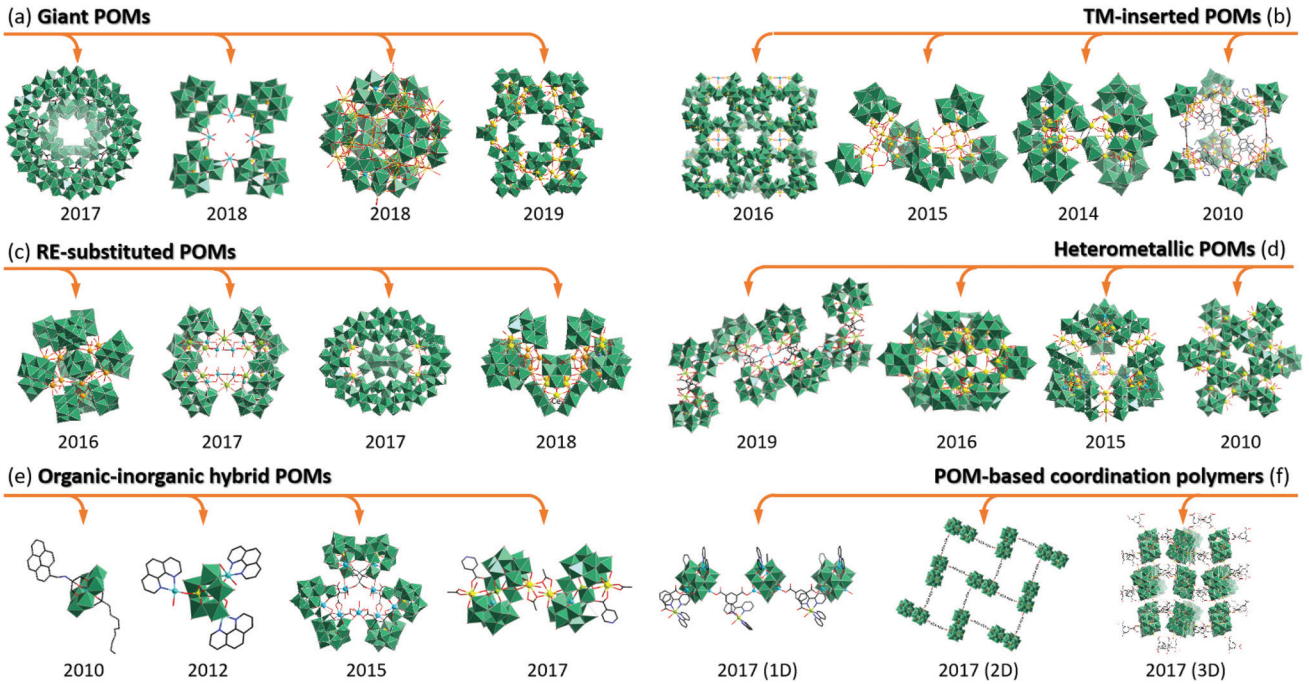

Fig. 2 (a) Combined ball-and-stick and polyhedral views of some typical inorganic giant POMs. (b) Combined ball-and-stick and polyhedral views of some typical TM-inserted POMs. (c) Combined ball-and-stick and polyhedral views of some typical RE-substituted POMs. (d) Combined ball-and-stick and polyhedral views of some typical TM-RE heterometallic POMs. (e) Views of some representative organic–inorganic hybrid POMs. (f) Views of some representative POM-based coordination polymers.[8,18,24–41]

(LOCSPHs), (3) POM-based double-material composites and (4) POM-based multi-material composites.

2.1 POMCPs

Owing to the negatively-charged surface and defect binding sites in so-called lacunary POM building blocks, POMs with various constituents, structures and sizes have shown great potential for constructing POMCPs *via* coordination bonds or even supramolecular interactions with organic ligands. These POMCPs with novel structures and enhanced properties open a new avenue for PCMs with highly ordered 1D, 2D or 3D topological structures. POMCPs are attracting intensive interest because of the enlarged pores and cavity sizes, tunable and robust crystal structures, and variable redox and adjustable acid–base properties endowed by POMs.[15] One of the most effective approaches to prepare POMCPs is the self-assembly strategy and manifold structures can be achieved by tuning POM building blocks and metal or organic linkers.[14–16,41,48] Based on the promising possibility of POMs acting as building units of hybrid materials, Dolbecq's group hydrothermally synthesized a series of POMCPs based on the mixed-valent $\{\varepsilon\text{-}PMo_8^{V}Mo_4^{VI}O_{40}Zn_4\}$ Keggin units, and diverse structures were achieved by choosing different organic linkers and counterions. This work further demonstrates for the first time that *in situ* replacement of common tetrabutylammonium counterions in ε-Keggin-based coordination polymers is possible and a totally new counterion might contribute to more attractive structures (Fig. 2f).[41] In addition, Wang and Zaworotko provided four unprecedented nanoscale Goldberg POMCPs exhibiting icosahedral geometries based on $[WV_5O_{11}(SO_4)_6]^{8-}$ clusters as the first pentagonal molecular building blocks (Fig. 3). The Goldberg POMCPs were obtained by solvothermal assembly of $[WV_5O_{11}(SO_4)_6]^{8-}$ with linear or triangular organic ligands, and the largest Goldberg $[(WV_5O_{11}SO_4)_{12}(TATB)_{20}]^{36-}$ shows a diameter of 4.3 nm.[48]

2.2 LOCSPHs

Introducing large organic cations by the cation exchange method to combine POM polyoxoanions to construct

Junwei Zhao

Junwei Zhao obtained his BS degree in chemistry in 2002 and obtained his MS degree under the supervision of Prof. Jingyang Niu in 2005 from Henan University. In 2008, he received his PhD under the supervision of Prof. Guo-Yu Yang at the Fujian Institute of Research on the Structure of Matter, Chinese Academy of Sciences. He is now a professor at the College of Chemistry and Chemical Engineering, Henan University. His current research mainly focuses on the synthesis and preparative chemistry of POM-based functional materials and the relevant optical, electric, magnetic and biological properties.

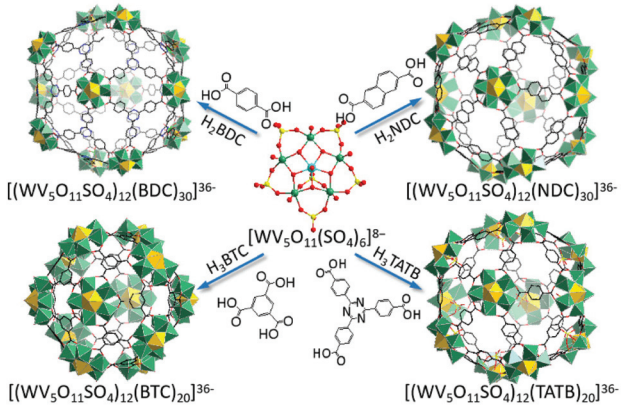

Fig. 3 Crystal structures of four nanoscale Goldberg POMCPs based on pentagonal $[WV_5O_{11}(SO_4)_6]^{8-}$ clusters.[48]

novel LOCSPHs *via* electrostatic interactions is another meaningful way to obtain better stability and application performances.

Ionic liquids (ILs) are substances entirely composed of ions and present a series of special properties, like high ionic conductivity, wide electrochemical stability and nonvolatility. Anions in ILs can be replaced by POM anionic clusters at room temperature, leading to the formation of POM-based ionic liquids (POM-ILs). As expected, POM-ILs possess significant reactivity and outstanding chemical versatility which can be tuned by chemical design.[49,50] Just as being demonstrated by Nagaiah and Mandal, a poly(vinyl butylimidazolium) (PVIM) stabilized cobalt-POM (CoPOM) composite material was prepared *via* cation exchange and the ionic polymer matrix, PVIM, provided a stable platform for CoPOM to display a significant electrocatalytic activity toward water oxidation (WO) (Fig. 4a).[49] Besides, surfactants with long hydrocarbon chains are also universally applied in POM modification, and surfactant encapsulation of POMs is a facile and effective way to solve the easy solubility of most POMs.[51] Notably, different from POM-ILs and surfactant encapsulated POMs, Polarz's group provided a unique family of organic–inorganic hybrid POM-surfactants (POMSURFs) containing lacunary $[PW_{11}O_{39}]^{7-}$ heads self-assembled with π-conjugated organo-alkoxysilanes as surfactant tails, and an electronic communication between heads and tails has been proved, thus further opening a new avenue for lyotropic and soft semiconductors (Fig. 4b).[52–57] Beyond acting as amphiphiles, such room-temperature obtained POMSURFs are catalytically active benefiting from the heteropolyacid head groups.[53,58]

2.3 POM-based double-material composites

2.3.1 Composites of POMs and metal-NPs. Metal (especially noble metals) NPs have demonstrated to be effective catalysts in many catalytic processes. However, the aggregation phenomenon largely hinders their further practical application. Loading an active POM species onto the surface of metal-NPs will provide the desired composites with better stability and performances, which has been certified by $[PMo_{12}O_{40}]^{3-}$ (PMo_{12}) anchored Pt NPs,[59] Ag NPs,[60] and Au NPs[61] (Fig. 5). Among the various available technologies (coating, immersing or deposition), electrolytic deposition and chemical deposition are deemed as the most effective routes to prepare highly-ordered POM-coated NPs. Specifically, metal NPs are acquired by the reduction of the corresponding high-valence metal salts *via* the electrochemical strategy[60] or the direct chemical method[61] in the presence of POMs, where POMs are absorbed on the surface of NPs and serve as stabilizing agents.

2.3.2 Composites of POMs and porous framework materials. Apart from working as building blocks in POMCPs,

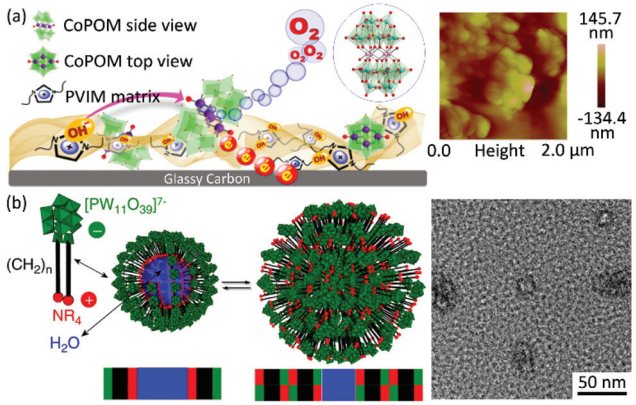

Fig. 4 (a) Schematic representation of the PVIM-CoPOM as an electrocatalyst for water oxidation (left) and the AFM image of the composite material (right).[49] (b) Schematic representation of the POMSURFs with a lacunary $[PW_{11}O_{39}]^{7-}$ head and a cationic ammonium tail and the self-assembly behavior at room temperature (left); and the temperature increase contributes to a structural transformation as well as a step-wise growth of the vesicles (middle); transmission electron microscopy (TEM) image of a dispersion of POMSURF vesicles containing *tert*-butyl (11-(triethoxysilyl)undecyl)carbamate attached to $[PW_{11}O_{39}]^{7-}$ (right).[55]

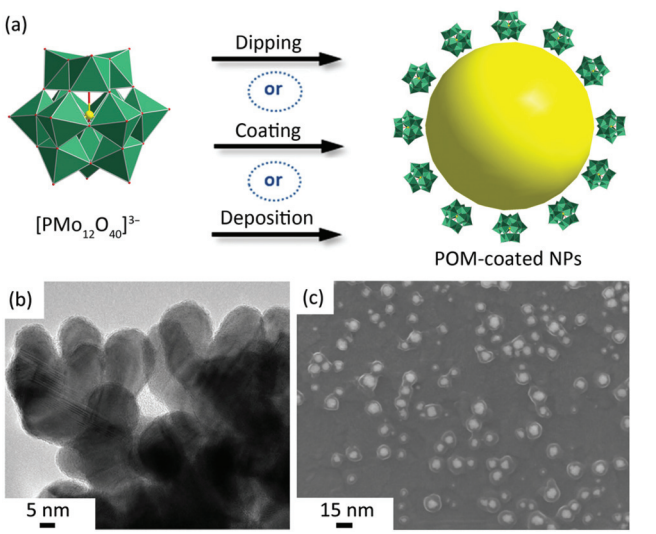

Fig. 5 (a) Schematic drawing of metal-NPs coated with PMo_{12}. (b) TEM image of Ag-PMo_{12} nanocomposites obtained by electrodeposition.[60] (c) Scanning electron microscopy (SEM) image of PMo_{12}-coated AuNPs.[61]

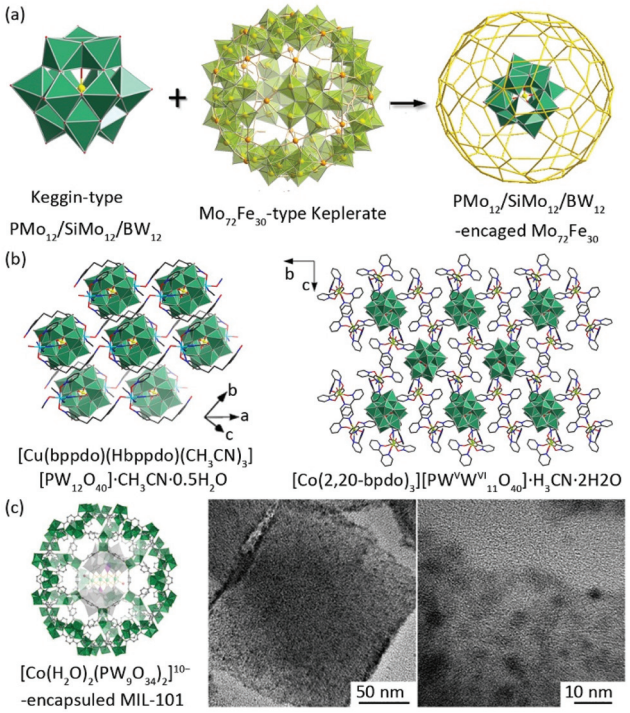

Fig. 6 (a) Schematic drawing of Keggin POMs ($PMo_{12}/SiMo_{12}/BW_{12}$) encaged in $Mo_{72}Fe_{30}$ Keplerate.[62] (b) The host–guest POM-templated supramolecular networks $[Cu(bppdo)(Hbppdo)(CH_3CN)_3][PW_{12}O_{40}]\cdot CH_3CN\cdot 0.5H_2O$ and $[Co(2,20\text{-}bpdo)_3][PW^{V}W^{VI}_{11}O_{40}]\cdot CH_3CN\cdot 2H_2O$.[63] (c) Proposed crystal structure and TEM images of $[Co(H_2O)_2(PW_9O_{34})_2]^{10-}$-encapsulated MIL-101(Cr).[64]

POMs can also serve as guest molecules to be immobilized into host porous materials such as self-assembly cages (*e.g.*, $PMo_{12}/[SiMo_{12}O_{40}]^{4-}$ ($SiMo_{12}$)/$[BW_{12}O_{40}]^{5-}$ (BW_{12}) encaged in $Mo_{72}Fe_{30}$ Keplerate cages, Fig. 6a),[62] supramolecular networks (*e.g.* $[Cu(bppdo)(Hbppdo)(CH_3CN)_3][PW_{12}O_{40}]\cdot CH_3CN\cdot 0.5H_2O$ and $[Co(2,20\text{-}bpdo)_3][PW^{V}W^{VI}_{11}O_{40}]\cdot CH_3CN\cdot 2H_2O$, Fig. 6b),[63] metal–organic frameworks (MOFs, *e.g.*, $[Co(H_2O)_2(PW_9O_{34})_2]^{10-}$ (ref. 64) and $[PMo_{10}V_2O_{40}]^{5-}$ (ref. 65) encapsulated in MIL-101(Cr), Fig. 6c) and zeolitic imidazolate frameworks (ZIFs, *e.g.*, $[CoW_{12}O_{40}]^{6-}$ (ref. 66) and $[PW_{12}O_{40}]^{3-}$/$[SiW_{12}O_{40}]^{4-}$/$[PMo_{12}O_{40}]^{3-}$ (ref. 67) enclosed in ZIF-8), to construct binary composites. POM-inserted porous framework materials are verified to display ameliorative activity and improved stability. The host–guest type POM-inserted framework materials can be facilely obtained by ion-exchange, mechanochemical synthesis, and a POM-template method.

2.3.3 Composites of POMs and carbon materials. Carbon materials (such as graphitic carbon, mesoporous carbon, CNT, graphene, graphene oxide (GO), reduced graphene oxide (rGO), and carbon quantum dots (CQDs)) have been widely studied due to their excellent electrochemical properties and conductivity. Depositing POMs on carbon surfaces (especially those activated by carboxylation, hydroxylation or alkylation) by chemical or electrolytic methods is a wise choice for gaining ideal composite materials. Dramatic enhancement of the electrochemical properties of composites of POMs and carbon materials is observed because of the area of the conductive surface enlarged by carbon materials and strong electronic communications between POMs and carbon materials. Therefore, carbon/POM composites undoubtedly present imponderable value in electrocatalysis,[68–72] electrochemical sensors,[73] fuel cells,[74] and so on. An outstanding work by Zhang and Kortz presented a novel binary nanocomposite composed of $[H_7P_8W_{48}O_{184}]^{33-}$ (P_8W_{48}) fixed on rGO sheets by a one-step electrochemical reduction synthesis, and P_8W_{48}/rGO was considered as a promising and low-cost hydrogen evolution reaction (HER) electrocatalyst (Fig. 7).[68]

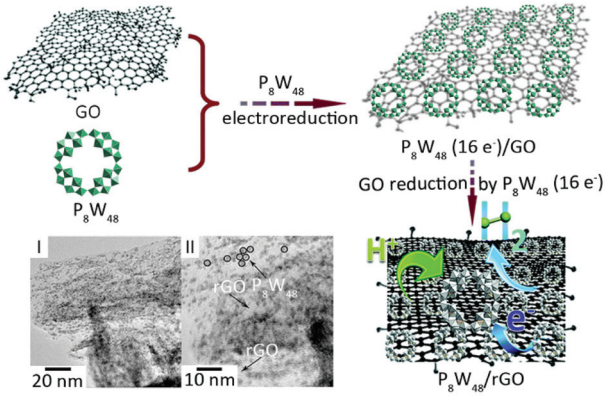

Fig. 7 Scheme of the one-step electrochemical reduction synthesis of the P_8W_{48}/rGO nanocomposite; TEM (I) and HRTEM (II) images of the as-prepared P_8W_{48}/rGO nanocomposite.[68]

2.3.4 POM-immobilized composite films. Preparing POM-immobilized films on suitable substrates[22,75–77] with controllable thickness is a significant way to obtain useful 2D materials with good stability, conductivity and practicability in practical devices. According to previous research, conducting polymers have been favored as substrate materials for a long time for their noteworthy conducting ability and easy molding *via* the physical method.[76,77] By virtue of the classic layer-by-layer (LbL) technique, which is based on the electrostatic interactions between oppositely charged species from dilute solution, some substrate candidates (especially glassy carbon[22,75]) have been reported. It is worth mentioning that the famous breath-figure-driven templating strategy has been verified to be applicative in POM systems since the nanoscale POMs have been testified as a valuable candidate for the construction of special honeycomb-patterned thin films by Hao and Liu.[78] Very recently, an ordered honeycomb structure of the surfactant-encapsulated POM (SEP) complex based on a sandwich type $K_7Na_3[Cu_4(H_2O)_2(PW_9O_{34})_2]\cdot 20H_2O$ ($Cu_4(PW_9)_2$) was successfully obtained after surface-encapsulation by a cationic surfactant dimethyldioctadecylammonium bromide (DODA·Br) through the breath figure method (Fig. 8), further revealing that ordered porous honeycomb films can be obtained by the self-assembly of surfactant-encapsulated magnetic POMs under a moist atmosphere. Furthermore, the effective electrocatalytic action of a honeycomb film modified indium tin oxide (ITO) electrode for the BrO_3^- reduction

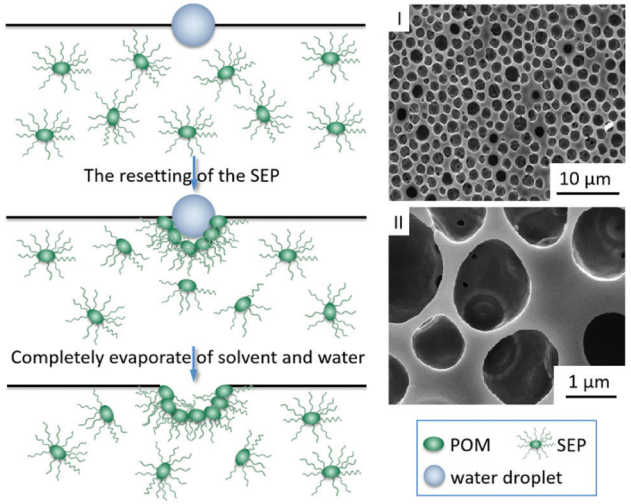

Fig. 8 Schematic view of the microporous honeycomb structure; SEM images of the as-prepared honeycomb-patterned hybrid films based on $Cu_4(PW_9)_2$ and DODA at low (I) and higher (II) magnification.[79]

offered a new idea for developing film materials in electrochemistry.[79]

2.4 POM-based multi-material composites

Combining the respective advantages of different materials, composites with more materials (usually triple-materials) have arisen, and each material works synergistically giving preeminent performances. Looking back at the previous studies in related fields, the more preferred PCMs are multi-component composites, in which POMs are composited with NPs, framework materials (*e.g.* MOFs, ZIFs), carbon materials and/or polymers.[80–92] A well-defined Au NP@POM-GN (POM: $H_3PW_{12}O_{40}$; GN: graphene nanosheet) nanohybrid was reported by Zhang *et al.* in 2012 (Fig. 9a) and POMs here not only are benefit to the $AuCl_4^-$ reduction process but also bridge NPs and GNs.[83] Whereafter, Yuan's group deposited PtPd NPs uniformly on the surface of multi-walled carbon nanotubes (MWCNTs) by the assistance of PMo_{12} and the size of PtPd NPs could be controlled by tuning their composition (Fig. 9b).[85] Lately, Liu and co-workers presented a ternary nanocomposite $[P_2W_{18}O_{62}]^{6-}/SnO_2$/Au NPs film *via* LbL self-assembly on ITO (Fig. 9c). The nanocomposite film shows a wide electrochemical determination range of myricetin from 1 to 110 μmol L^{-1} compared to other reported electrodes, and an extraordinary electrocatalytic activity was achieved by the synergetic contribution of the synergistic effect of P_2W_{18} with multi-electron reversible electrocatalytic properties, mesoporous SnO_2 with high conductivity and an electroactive surface area, and AuNPs with outstanding conductivity and electrocatalytic properties.[90] As is reported, the preparation strategies mentioned above and stepwise synthesis combining different methods are applicable for multi-material composites. Noteworthily, POMs play a key role in the multi-component composites, which often serve as reductants for reduced metal NPs or GO, encapsulating molecules (stabilizer) of NPs, as well as bridging molecules between different materials.[83–85] In such a multicomponent system, different components work synergistically to achieve more splendid performances in catalysis,[80–82,84–89,91] detection[83,90] or other fields.

3. Electrochemical applications of POMs and PCMs

The electrochemical behaviors of POMs are captivating since many POMs can undergo a fast, reversible and stepwise multi-electron transfer reaction with keeping their structures unchanged.[93] Thus, electrochemically active POMs and PCMs are favored in the fields of proton conductivity, electrocatalysis and electrochemical sensing and increasing attention has been paid on related investigations in the past decade (Fig. 10). Furthermore, the most studied POMs are Keggin-type ($XM_{12}O_{40}^{n-}$) and Dawson-type ($[X_2M_{18}O_{62/60}]^{n-}$) (X = heteroatoms,

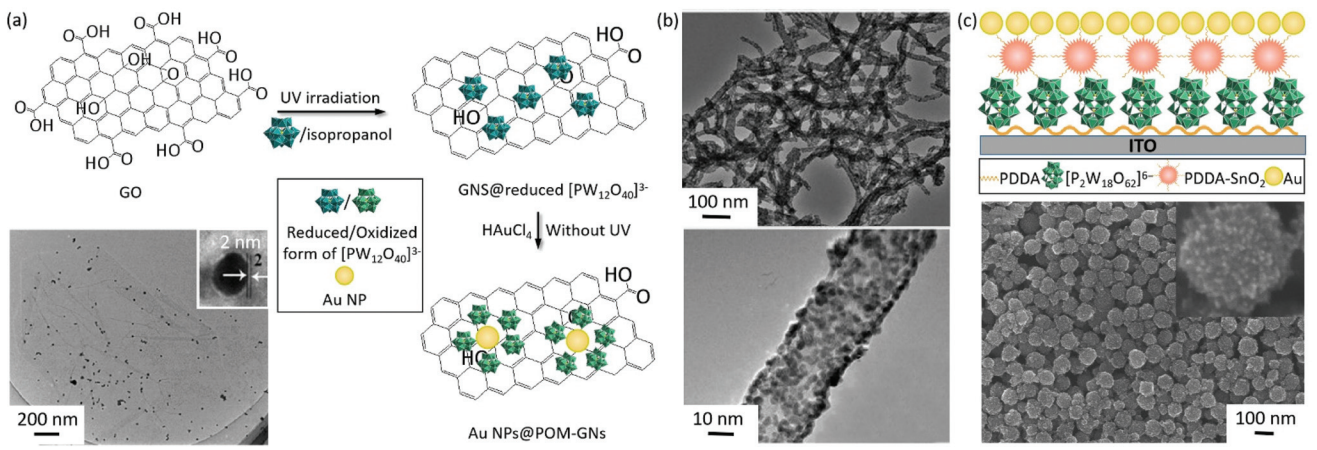

Fig. 9 (a) Preparation procedure of Au NP@POM-GN nanohybrids and the TEM image of the as-prepared composite.[83] (b) TEM images of $[PMo_{12}O_{40}]^{3-}/Pt_8Pd_1$/MWCNTs.[85] (c) Schematic representation (up) and the SEM image (down) of the $[P_2W_{18}O_{62}]^{6-}$-SnO_2-AuNP multilayer film on an ITO electrode.[90]

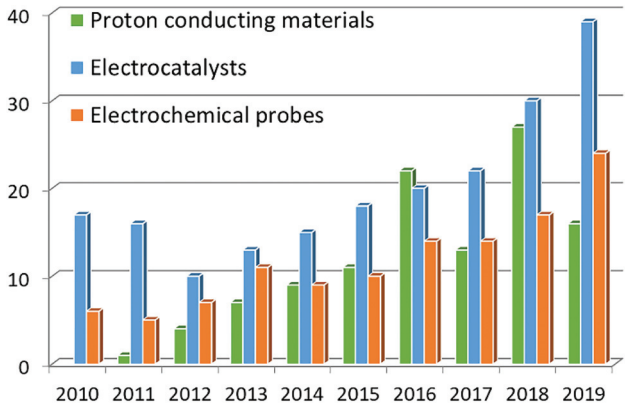

Fig. 10 Representative articles about POMs and PCMs applied as electrocatalysts, electrochemical detection probes and proton conducting materials published in the past decade.

such as P^{V}, $As^{III/V}$, Si^{IV}, Ge^{IV}, Sb^{III}, Se^{IV} or Te^{IV}), which is mainly due to their considerable stability. The latest research advances in POMs and PCMs as proton conducting materials, electrocatalysts and electrochemical detection probes will be emphatically introduced in the following aspects.

3.1 Proton conducting materials

Since the proton conductivity of the phosphotungstic acid ($H_3PW_{12}O_{40}\cdot 28H_2O$) was first reported by Nakamura in 1979,[94] POMs and PCMs with high proton conductivity have been universally pursued and have shown great potential in electrochemical device fabrication and fuel cells.[38]

Remorseless efforts have been devoted to constructing fresh POM-based proton conducting materials. Notably, in the work of Zhao, Carsten and Song, the first giant cerium–bismuth tungstate cluster $Na_{16}(NH_4)_{10}H_8$ $\{[W_{14}Ce^{IV}_6O_{61}]([W_3Bi_6Ce^{III}_3(H_2O)_3O_{14}][\alpha\text{-}BiW_9O_{33}]_3)_2\}\cdot ca.\ 38H_2O$ was synthesized by a one-pot self-assembly, while trivalent Bi^{3+} cations were used together with RE cations to link and stabilize the giant tungstate clusters. Water-filled channels with the diameter of *ca.* 0.5 nm in the structure contributes to a good proton conductivity of 4.9×10^{-7} S cm^{-1} at −40 °C with structural integrity.[33] Furthermore, novel POM-organic supramolecular nanotubes have proved to be outstanding proton-conducting materials. Rare inorganic–organic hybrid supramolecular nanotubes $[H_2en]_4[Ni_5(OH)_3(trzS)_3(en)(H_2O)(B\text{-}\alpha\text{-}PW_9O_{34})]\cdot 6H_2O$ (en = ethylenediamine) (Fig. 11a)[95] and $[Cu_3(\mu_3\text{-}OH)(H_2O)_3(atz)_3]_3[P_2W_{18}O_{62}]\cdot 14H_2O$ (Hatz = 3-amino-1,2,4-triazolate)[96] behave as outstanding proton conductors (2.4×10^{-4} S cm^{-1} at 98.0% relative humidity (RH) and 85 °C, and 4.4×10^{-6} S cm^{-1} at 97% RH and 25 °C, respectively), pointing out a new direction for the development of proton conducting materials. Compared with traditional metal–organic nanotubes (MONTs), POM-based MONTs, in which POMs serve as linkages between neighboring MONTs through covalent bonds, have presented more attractive stability and proton conductivity.

Moreover, PCMs are supposed to be benefited from each component working synergistically. In Liu's work in 2014, $H_3PW_{12}O_{40}$ was introduced into the framework (HKUST-1) and the resulting product $[Cu_{12}(BTC)_8(H_2O)_{12}][H_3PW_{12}O_{40}]\cdot nH_2O$ features uniform proton-conducting pathways in three orthogonal directions, showing increased proton conductivity by 5 orders of magnitude compared to that of the parent HKUST-1.[97] As a result, POMs are believed to be an excellent modifier to adjust the conductivity of MOFs (Fig. 11b). Furthermore, Luo and Liu reported a $H_3PW_{12}O_{40}$-modified sponge-like GO monolith (PEGO) with a 3D crosslinking inner structure in 2015.[98] Owing to the introduction of $[PW_{12}O_{40}]^{3-}$ and the replacement of unstable epoxy groups by ethylenediamine, PEGO exhibits an ultra-high proton conductivity under low RH (1.02×10^{-2} S cm^{-1} under 80 °C at 60% RH) and excellent long-term stability (more than 1 month). The outstanding conductivity originates from 3D transporting pathways, high-density hopping sites and eliminated grain boundary resistance (Fig. 11c).[98]

Taking advantage of MOFs (another proton conductor) and Strandberg $[Mo_5P_2O_{23}]^{6-}$ clusters, the first proton conducting Strandberg POM-organic framework (POMOF) $[Mo_5P_2O_{23}][Cu(phen)(H_2O)]_3\cdot 5H_2O$ was obtained by Banerjee's group in 2012.[38] Due to parallel water chains in the network, this composite exhibits excellent proton conductivity (2.2×10^{-5} S cm^{-1} at 301 K with 98% humidity) in the solid state. In 2016, Xu and Bu provided the first gyroidal POMOF $\{Na_7[(n\text{Bu})_4N]_{17}\}[Zn(P_3Mo_6O_{29})_2]_2\cdot xG$ (G = guest solvent molecules), constructed by a rare pair of chiral $[P_3Mo_6O_{31}]^{11-}$ enantiomers and zinc ions.[27] This compound reveals a high proton conductivity of

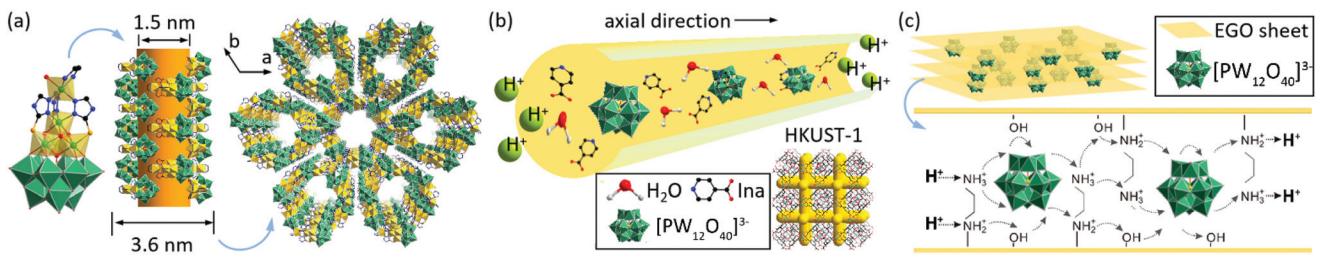

Fig. 11 (a) Structure of the $[Ni_5(OH)_3(trzS)_3(en)(H_2O)(B\text{-}\alpha\text{-}PW_9O_{34})]^{8-}$ anion, and the side/top view of the nanotubular structure of the inorganic–organic hybrid supramolecular $[H_2en]_4[Ni_5(OH)_3(trzS)_3(en)(H_2O)(B\text{-}\alpha\text{-}PW_9O_{34})]\cdot 6H_2O$.[95] (b) Schematic of the uniform proton-conducting pathway constructed using $H_3PW_{12}O_{40}$, isonicotinic acid (Ina) and water molecules arranged alternately in the nano-channels in HKUST-1.[97] (c) Proposed mechanism for proton conductivity in the PEGO monolith (EGO: EN-functionalized GO).[98]

1.04×10^{-2} S cm^{-1} at 75% RH (80 °C) resulting from the proton carriers (like water, Na^+ and $[(Bu)_4N]^+$, *etc.*) in the resultant gyroidal channels. Meanwhile, the as-prepared material also exhibits electrocatalytic activity toward the reduction of nitrite.

A Preyssler-type POM $[Bi(H_2O)P_5W_{30}O_{110}]^{12-}$ was recently studied in the proton conducting field by crystallization with potassium ions and poly(allylamine).[99] The results demonstrate that the side-chain mobility of the poly(allylamine) and hydrogen-bonding network is contributed by the proton conduction of the compound with poly(allylamine), achieving a proton conductivity of 10^{-2} S cm^{-1} under mild-humidity and low-temperature conditions.[99]

3.2 Electrocatalysts

Some appealing characteristics of POMs have been verified: (1) their redox potential can be adjusted by changing heteroatoms or coordination atoms without affecting their structures, (2) TM cations in heteropolyoxometalates (HPOMs) are polytropic, and (3) multielectron transfer is possible. These make POMs attractive for electrochemical processes as catalysts with high performance, especially HPOMs, in which the average potential of the first redox pairs increases linearly with an increase in the valence of the central heteroatom, *i.e.*, a decrease in the negative charge of the heteropolyanions.[100]

Keggin-type POMs are regarded as the most robust structural units among all POMs. Keggin-type and Keggin-like POMs and various hybrids with NPs, porous materials, carbon materials, nickel foam and so on, have been extensively studied as electrocatalysts for carbon dioxide reduction, the oxygen evolution reaction (OER), and the reduction of bromate, persulfate, nitrite, *etc.* Specifically, some representative findings will be described.

Pursuing POMs with novel structures is a promising way for electrocatalyst exploration. In 2015, Zhang and Mialane *et al.* acquired a novel bisphosphonate-bridging heptanuclear Ni^{II} core sandwiched phosphotungstate $[\{(B\text{-}PW_9O_{34})Co_3(OH)(H_2O)_2[O_3PC(O)\{C_3H_6NH_2CH_2(C_5NH_5)\}PO_3]\}_2Co]^{12-}$ ($Co_7(AlePy)_2$), which can be further used as a precursor for heterometallic (Zn, Pd and Pt) hybrid compounds.[101] The composite of metal-free $Co_7(AlePyZn)_2$ and the carbon material, for the first time, represents a low-cost oxygen reduction catalyst in a four-electron process and illustrates good performance, high selectivity, long-term stability and outstanding tolerance to the crossover effect, even in neutral media (Fig. 12a).[101] Another research by Niu and Wang proposed a trimeric ruthenium-substituted isopolyoxotungstate based on the Keggin-like $\{Ru_{1.83}W_{10.17}\}$ building blocks, $Rb_{10}K_3H_6[SeO_3(H_9Ru^{IV}_{5.5}W_{30.5}O_{114})]Cl_3{\cdot}48H_2O$, which is not only the first example of inorganic Ru-POMs based on isopolytungstates, but also a rare example of SeO_3^{2-}-bridging trimeric structures, demonstrating electrocatalytic activity toward the nitrite oxidation reaction in aqueous solution (Fig. 12b).[102]

In Lan's work, a series of POM-metalloporphyrin organic frameworks (PMOFs) were made and $[PMo^V_8Mo^{VI}_4O_{35}(OH)_5Zn_4]_2[MTCPP][2H_2O][1.5TBAOH]$ (M = Fe, Co, Ni, and Zn) is constructed from tetrakis[4-carboxyphenyl]-porphyrin-M (M-TCPP) ligands and reductive Zn-ε-Keggin clusters by the hydrothermal method.[103] Notably, the integration of $\{\varepsilon\text{-}PMo^V_8Mo^{VI}_4O_{40}Zn_4\}$ clusters and metalloporphyrin ligands endows these PMOFs with excellent performance in electrochemical carbon dioxide reduction (ECR) by taking advantage of electron collection and donation, electron migration and electrocatalytically active components. In particular, the best faradaic efficiency of the Co-PMOF can reach up to 99% (highest in reported MOFs), and the Co-POM presents a high turnover frequency (TOF) of 1656 h^{-1} and an excellent catalysis stability (>36 h) (Fig. 12c).[103] Coincidentally, Keggin-type PMo_{12} anchored Ag NPs (Ag-PMo_{12}) have also shown high catalytic activity for ECR in a water–DMF system according to Zhang's research.[60] Significantly, it has demonstrated that POMs could reduce the overpotential for CO_2 reduction and enhance the current density, being served as more attractive catalyst candidates.[60]

In 2018, Das and coworkers reported two significant research studies on POM-based composites as electrochemical water oxidation catalysts (WOCs).[104] One is a POM-supported nickel(II) coordination complex, $[Ni^{II}(2,2'\text{-bpy})_3]_3[\{Ni^{II}(2,2'\text{-bpy})_2(H_2O)\}\{HCo^{II}W^{VI}_{12}O_{40}\}]_2{\cdot}3H_2O$ (2,2′-bpy = 2,2′-bipyridine). The catalytic process accompanies a proton-coupled electron transfer pathway (two electrons and one proton) with Ni^{II} ions (coordinated to the POM surface) as the active centers and no formation of metal oxide in the process, and the TOF was 18.49 (mol of O_2)(mol of Ni^{II})$^{-1}$ s^{-1}. More importantly, this is the first report of a hybrid containing POMs as inorganic units and 2,2′-bpy ligands as organic units linked together with Ni^{II} ions (Fig. 12d). Another WOC is the POM@ZIF-8 composite obtained by the confinement of the first plenary Keggin anion $[CoW_{12}O_{40}]^{6-}$ in the well-defined void space of ZIF-8.[66] The POM@ZIF-8 catalyst had a TOF of 10.8 mol O_2(mol Co)$^{-1}$ s^{-1}, one of the highest TOFs for electrocatalytic oxygen evolution at neutral pH. Furthermore, the initial activity was still maintained even after 1000 cycles, which is attributed to the good size match between the host (ZIF-8) and the guest (Keggin anions), which prohibits the release of the $[CoW_{12}O_{40}]^{6-}$ unit from the smaller windows (3.4 Å) in ZIF-8 once put inside by the *in situ* synthesis.

Moreover, great attention has also been paid on Dawson-type POM-based electrocatalysts in the past ten years. Typically, an organic–inorganic heteropoly blue, $(MB)_5[S_2Mo^V_1Mo^{VI}_{17}O_{62}]{\cdot}CH_3CN$ (MB = $C_{16}H_{18}N_3S$), was researched by Xue in 2013.[100] With S^{VI} as the central heteroatom, the Dawson-type polyanions are fascinating owing to the most excellent electron acceptability (for example, $[S_2Mo_{18}O_{62}]^{4-}$ can accept up to 26 electrons). As respected, this compound displays high stability and good electrocatalytic activity toward the reduction of nitrite, chlorate, bromate and hydrogen peroxide in acidic (1 M H_2SO_4) aqueous solution when being immobilized on a modified carbon paste electrode (CPE).[100] In 2014, McCormac *et al.* prepared a tetra Ru-substituted $Na_{10}[\{Ru_4O_4(OH)_2(H_2O)_4\}(\gamma\text{-}SiW_{10}O_{36})_2]$ (Ru_4POM) POM-based LbL film with stability and reproducibility on a glassy carbon electrode (GCE) or ITO coated glass by employing a

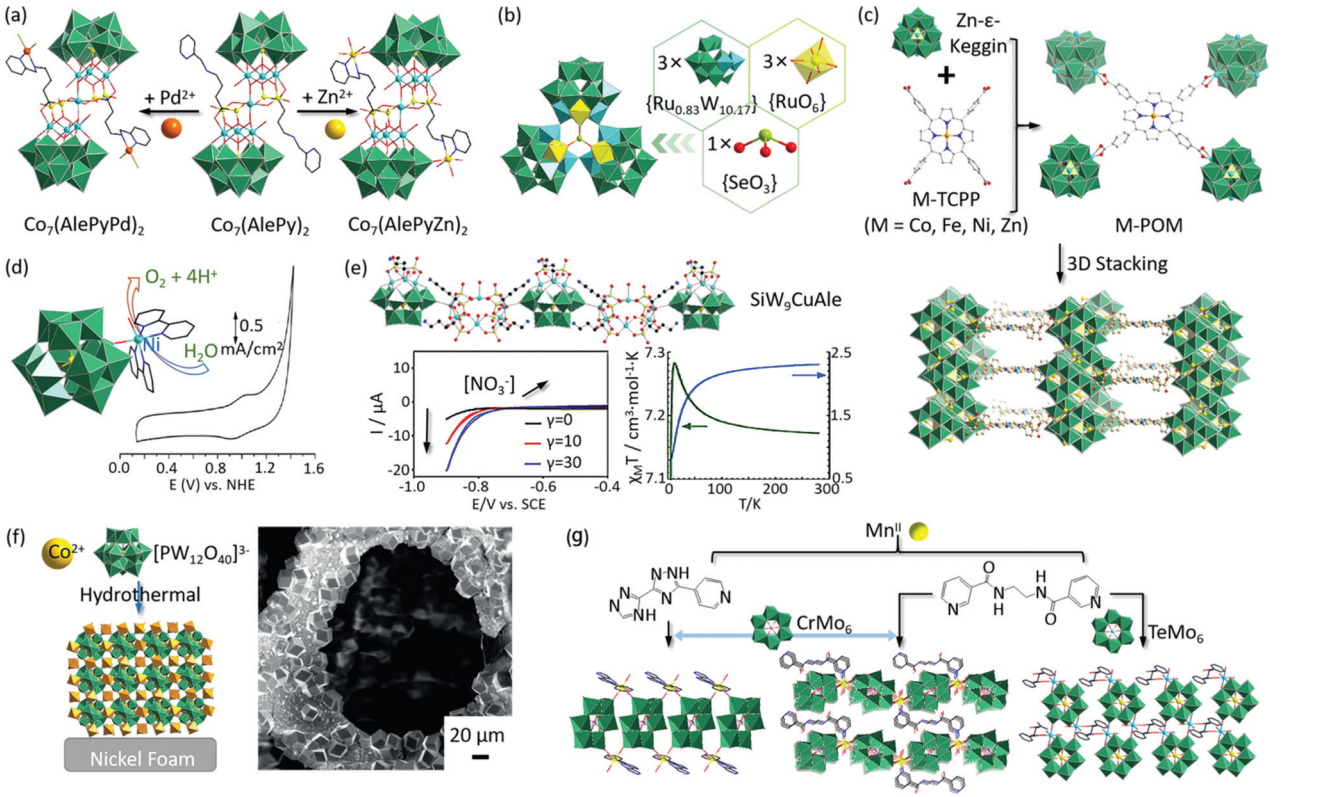

Fig. 12 (a) Mixed polyhedral and ball-and-stick representations of the polyanionic unit in $Co_7(AlePyZn)_2$ and $Co_7(AlePyPd)_2$.[101] (b) Top view and side view of the ball-and-stick and polyhedral representations of the polyanion $[SeO_3(H_9Ru^{IV}_{5.5}W_{30.5}O_{114})]^{16-}$.[102] (c) Schematic illustration of the structures of M-PMOFs (M = Co, Fe, Ni, Zn).[103] (d) Structure of the asymmetric unit of compound D1 (H atoms are omitted for clarity) and thermal ellipsoids are set to the 50% probability level.[104] (e) Crystal structure of SiW_9CuAle (up) and its significant activity upon the reduction of NO_3^-.[106] (f) Deposition of Dexter–Silverton POM microcrystals on nickel foam electrodes and the high-magnification SEM image of the NiCo-POM/Ni electrode.[107] (g) Structures of the title POMCPs constructed from Anderson-type XMo_6 (X = Cr/Te), Mn^{II} atoms and different pyridyl-derivative ligands through hydrothermal synthesis.[108]

Ru(II)-metallodendrimer as the cation. The homogeneous films show noteworthy stability even when the pH varies from 2 to 5 and are quite porous with good permeability towards the redox probes, providing enhanced electrocatalytic performance to WO in phosphate buffered saline (pH = 7).[76]

Vagin's group presented a series of LbL films composed of Dawson-type mono-TM substituted heteropolyanions (HPAs) α_2-$[P_2W_{17}O_{61}M]^{8-}$ (M = Fe^{III} and Ni^{II}) and silver NPs, exhibiting electrocatalytic properties towards both the nitrate reduction reaction (NRR) and nitrite reduction in mild acidic media (pH 4.5), while TM-substituted HPAs with electrocatalytic activity towards the NRR in mild acidic media are rarely reported.[105] Increasing TM centers within the HPA cages favors the enhancement of the catalytic properties of these atoms. Later, Ruhlmann and Mialane for the first time reported three polyoxotungstates containing multi-Cu^{2+} ions and bisphosphonate ligands $Na_{12}[\{SiW_9O_{34}Cu_3(Ale)(H_2O)\}\{Cu_6(Ale)_4(H_2O)_4\}]\cdot 50H_2O$ (SiW_9CuAle), $Na_8Li_{29}[\{(SbW_9O_{33})_2Cu_3(H_2O)_{2.5}Cl_{0.5}\}_2\{Cu_6(Ale)_4(H_2O)_4\}_3]\cdot 163H_2O$ (SbW_9CuAle) and $Na_{20}[\{(P_2W_{15}O_{56})_2Cu_4(H_2O)_2\}\{Cu_6(Ale)_4(H_2O)_4\}]\cdot 50H_2O$ ($P_2W_{15}CuAle$) (Ale = alendronate) (Fig. 12e).[106] These POMs show an outstanding electrocatalytic performance for the reduction of nitrites (HNO_2 or NO_2^-), while SiW_9CuAle and $P_2W_{15}CuAle$ also exhibit a significant activity upon the reduction of nitrate (NO_3^-), evidencing that the $[Cu_6(Ale)_4(H_2O)_4]^{4-}$ cluster plays a crucial auxiliary role in significantly enhancing the catalytic efficiency of the active POM matrixes.

Besides the most reported Keggin- and Dawson-type POMs, some other type POMs were also investigated as electrocatalysts. Streb and Song addressed an interesting work on a robust Dexter–Silverton POM, ($[Co_{6.8}Ni_{1.2}W_{12}O_{42}(OH)_4(H_2O)_8]$) oxygen evolution catalyst (POM-OEC) immobilized on a commercial nickel foam electrode by a facile one-step hydrothermal route, as the first stable POM used in alkaline (pH 13) water electrolysers.[107] The electrode indicates electrochemical oxygen evolution at low overpotential (360 mV at 10 mA cm^{-2} against the reversible hydrogen electrode (RHE), a Tafel slope of 126 mV dec^{-1}, and a faradaic efficiency of (96 ± 5)%) without chemical or mechanical degradation (Fig. 12f).[107] Besides, three unprecedented Anderson-type POMCPs ($[Mn_2(4\text{-pdtz})_2[CrMo_6(OH)_5O_{19}](H_2O)_4]$, $\{Mn(3\text{-dpye})_{0.5}[CrMo_6(OH)_6O_{18}](H_2O)\}\cdot(3\text{-}H_2dpye)_{0.5}$ and $[Mn_2(3\text{-}H_2dpye)(TeMo_6O_{24})(H_2O)_6]\cdot 4H_2O$ (4-pdtz = 4-pyridinobistriazol, 3-dpye = *N*,*N*′-bis(3-pyridinecarboxamide)-1,2-ethane) were communicated in 2017,

pointing out the crucial role of organic ligands and the center Mn^{II} ions in tuning the dimensionalities and structures of POMCPs.[108] Furthermore, $[Mn(4\text{-pdtz})_2[CrMo_6(OH)_5O_{19}](H_2O)_4]$ is considered as the first example of Anderson POM-based POMCPs derived from the bis-triazole ligand. All the obtained complexes exhibit excellent electrocatalytic activity toward the reduction of bromate and hydrogen peroxide (Fig. 12g).[108]

3.3 Electrochemical probes

The applications of POMs in electrochemical recognition are mainly based on their multielectron redox properties resulting in fast and selective response in amperometric measurements. Until now, electrochemical detection of inorganic[73,109–113] and biomolecules[74,90,112,114–117] has been achieved.

Transition metal NPs and various carbon materials are the most commonly used candidates for preparing PCMs due to the excellent catalytic performance of TMs and the outstanding conductivity of carbon materials. In such composites, POMs are usually used as both reductants and bridging molecules. For example, the novel Au NPs@POMs/ordered mesoporous carbon composite materials (Au@$[PW_{12}O_{40}]^{3-}$/OMC) manifest fast electrochemical response toward acetaminophenol (AP), H_2O_2 and nicotinamide adenine dinucleotide (NADH) detection and could be further used as an enzyme-free biosensor (Fig. 13a).[112] Combining the advantages of Au NPs and OMC materials, such novel nanohybrids provide new features of electrocatalytic activities.

Developing splendid substrates for POM loading has always been an interesting topic in the related fields. Recently, Wang *et al.* studied a novel electrochemical sensor based on ZrO_2 NP loading with PON $(NH_4)_5PV_8Mo_4O_{40}$ (NPVMo) units on the GCE. The NPVMo-ZrO_2 nanocomposite was used in double signal amplification for the simultaneous detection of clenbuterol (CLB) and ractopamine (RAC) with high stability and electrocatalytic activities, and low limits of detection of 5.03×10^{-9} mol L^{-1} for CLB and 9.3×10^{-7} mol L^{-1} for RAC, as well as a wide range for calibration curves of CLB and RAC from 0.1 to 1000 μM and 3.0 to 50 μM, respectively.[117] In this work, ZrO_2, deposited with NPVMo was used as a POM carrier for the first time to prepare electrochemical sensors.

The great biocompatibility of POMs makes them precious in electrochemical biosensors. A series of distinguishing ala-decorated (ala = L-alanine) RE-containing arsenotungstates (RECATs) $[H_2N(CH_3)_2]_{12}Na_2H_2[Eu_4W_5(H_2O)_{10}(ala)_3O_{14}(As_2W_{19}O_{68})_2]\cdot 35H_2O$, $[H_2N(CH_3)_2]_{13}Na_3H_2[Tb_4W_6(H_2O)_8(ala)_4O_{15}(OH)_2(As_2W_{19}O_{68})_2]\cdot 36H_2O$ and $[H_2N(CH_3)_2]_{12}Na_4H_2[Ho_4W_6(H_2O)_{10}(ala)_2O_{15}(OH)_2(As_2W_{19}O_{68})_2]\cdot 40H_2O$ (Fig. 13b) were fabricated by Zhao's group in a facile one-step assembly strategy.[118] These as-synthesized RECATs as the modified electrode materials were utilized to manufacture CS-CMWCN-RECAT/GCE electrochemical sensors (CS = chitosan, CMWCNs = carboxyl functionalized multi-walled carbon nanotubes) and their electrochemical sensing properties toward dopamine detection were firstly evaluated and the electrochemical response mechanism was also provided, which may offer a hopeful perspective of RE-containing POMs for serving as electrochemical response electrode materials for realizing the detection of small biomolecules.[118]

Apart from Keggin-type POMs, Dawson-type POMs have also been used in biosensing. In 2018, Holzinger reported two inorganic–organic composites prepared by Dawson-type $(C_4H_{10}N)_6[P_2Mo_{18}O_{62}]\cdot 4H_2O$ (P_2Mo_{18}) and $(C_6H_8NO)_4[H_2P_2W_{18}O_{62}]\cdot 6H_2O$ (P_2W_{18}) nanoclusters confined in 1-pyrenemethylamine (PMA)

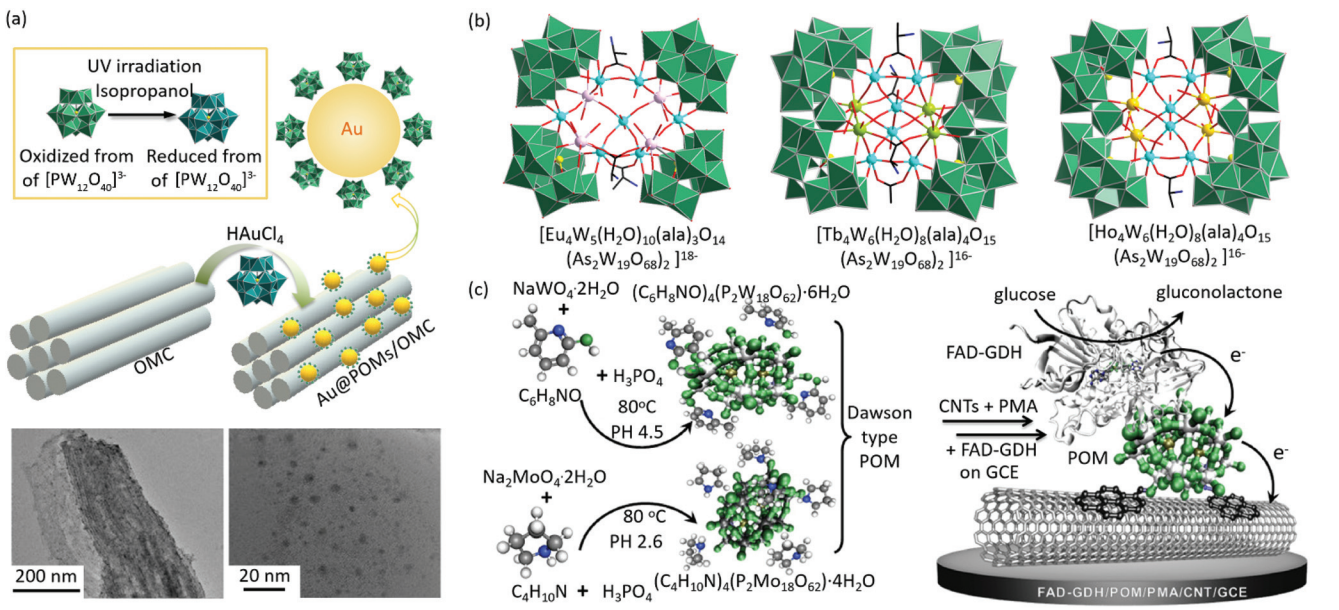

Fig. 13 (a) Illustration of the preparation and SEM images of Au@$[PW_{12}O_{40}]^{3-}$/OMC tri-component nanohybrids.[112] (b) Crystal structures of three ala-decorated RE-substituted POMs.[118] (c) Schematic diagram of the Dawson-type POMs (P_2Mo_{18}/P_2W_{18}) and PMA functionalized CNTs, and SEM images of P_2Mo_{18}/PMA/MWCNTs and P_2W_{18}/PMA/MWCNTs.[74]

functionalized CNTs, and the two composites could be further applied as bioelectrodes for glucose biosensors benefiting from POMs' promising redox behavior in a potential range for mediated electron transfer with the glucose oxidizing enzyme (Fig. 13c).[74]

In addition, a multilayer film consisting of crown-shaped phosphotungstate $K_{28}Li_5H_7P_8W_{48}O_{184}\cdot 92H_2O$ (P_8W_{48}) and CS as a cationic layer was obtained using an electrostatic LBL self-assembly technique, and displays excellent amperometric sensing performance for electro-detection of H_2O_2 with high sensitivity (0.53 mA mM^{-1}) and a low detection limit (1.3 μM) in a wide pH range from 1 to 8.[112] Moreover, a nanocomposite film based on P_8W_{48}, poly(ethylenimine) (PEI) modified rGO and Au NPs ({PEI/rGO}-Au@P_8W_{48}) was successfully fabricated by an electrochemical reduction technique, in which reduced P_8W_{48} acted simultaneously as a reducing agent, a stabilizer and bridging molecules.[72] This nanocomposite film was examined as the electrochemical probe to recognize H_2O_2 based on a high catalytic reduction activity with great sensitivity and selectivity, a low detection limit and a wide linear range.[73]

4. Conclusion and outlook

After a long period of development, PCMs are becoming an important class of promising smart candidates for functional materials in various applications derived from their glorious electrochemical performances. This review mainly focuses on the advances of POMs and PCMs in electrochemistry in the past decade. As is well known, exploring new materials with better stability, activity, and proton and electron conductivity is always imperative in practical applications, and is also believed to be the future development direction of POM science. Based on numerous previous findings, increasing attention should be paid on the following aspects:

(1) Manufacturing novel POM derivatives with unique structures by introducing different metal components is a crucial driving force in POM chemistry in order to find much more useful candidates used for exploiting excellent functional smart materials. Specifically, high-nuclear TM ions or even hetero-nuclear TM substituted POMs will facilitate more splendid catalytic performances on account of a synergistic effect of multicentric TM centers within the POM cages and the outstanding electron and proton transfer capacity of the POM skeletons. Therefore, future research will be concentrated on developing environmental-friendly catalysts in energy (*e.g.* HER) and environmental restoration (*e.g.* WO, NRR). Furthermore, smart materials combining optical (especially fluorescence) and electrical properties have long been a key research topic which is supposed to be achieved by introducing RE ions and excellent conductive components (for example, CNTs, rGO and CQDs) into POM systems.

(2) Organic–inorganic hybrid POMs are another eye-catching field in new material development. Most available POMs are modified by single organic ligands (either rigid ligands containing benzene ring or flexible ligands), leaving a lot of room to develop hybrid materials simultaneously modified with mixed ligands. Different organic components may provide different coordination modes to construct more amazing structures, which will potentially exhibit unexpected performances.

(3) Searching appropriate preparation strategies of compositing new POM-based candidates with other excellent electrochemical active materials to construct ideal performance-enhanced and multi-functional smart PCMs will call for increasing considerations with social and technological development requirements.

(4) Combination or complexity of PCMs with biological medicines to make application-oriented intelligent devices may produce many growth points for driving the applications of PCMs in materials chemistry, bioscience, clinical medicine and cancer detection in the future.

Abbreviations

POMs	Polyoxometalates
TMs	Transition metals
RE	Rare earth
PCMs	POM-based composite materials
NPsv	Nanoparticles
CNTs	Carbon nanotubes
POMCPs	POM-based coordination polymers
LOCSPHs	Large organic cation stabilized POM hybrids
TEM	Transmission electron microscope
ILs	Ionic liquids
POM-ILs	POM-based ionic liquids
PVIM	Poly(vinylbutylimidazolium)
CoPOM	Cobalt-POM
WO	Water oxidation
POMSURFs	POM-surfactants
MOFs	Metal–organic frameworks
ZIFs	Zeolitic imidazolate frameworks
SEM	Scanning electron microscope
GO	Graphene oxide
rGO	Reduced graphene oxide
CQD	Carbon quantum dot
HER	Hydrogen evolution reaction
LBL	Layer-by-layer
SEP	Surfactant-encapsulated POM
DODA	Dimethyldioctadecylammonium
GNS	Graphene nanosheets
MWCNTs	Multi-walled carbon nanotubes
ITO	Indium tin oxide
en	Ethylenediamine
Hatz	3-Amino-1,2,4-triazolate
Ina	Isonicotinic acid
EGO	EN-functionalized GO
PEGO	POM-modified sponge-like GO monolith
RH	Relative humidity
POMOFs	POM-organic frameworks
HPOMs	Heteropolyoxometalates

OER	Oxygen evolution reaction
WOC	Water oxidation catalysts
2,2′-bpy	2,2′-Bipyridine
PMOFs	POM-metalloporphyrin organic frameworks
ECR	Electrochemical carbon dioxide reduction
TOF	Turnover frequency
CPE	Carbon paste electrode
HPA	Heteropolyanion
NRR	Nitrate reduction reaction
GCE	Glassy carbon electrodes
OEC	Oxygen evolution catalyst
RHE	Reversible hydrogen electrode
AP	Acetaminophenol
NADH	Nicotinamide adenine dinucleotide
4-pdtz	4-Pyridino-bistriazol
3-dpye	*N*,*N*′-Bis(3-pyridinecarboxamide)-1,2-ethane
OMC	Ordered mesoporous carbon
CLB	Clenbuterol
RAC	Ractopamine
CS	Chitosan
CMWCNs	Carboxyl functionalized multi-walled carbon nanotubes
PMA	Pyrenemethylamine
ala	L-Alanine
PEI	Poly(ethylenimine)
RECATs	RE-containing arsenotungstates
MONTs	Metal–organic nanotubes

Conflicts of interest

There are no conflicts to declare.

Acknowledgements

This work was supported by the National Natural Science Foundation of China (21671054, 21871077, 21571048, 21771052), the Program for Innovation Teams in Science and Technology in Universities of Henan Province (20IRTSTHN004) and the Program of First-Class Discipline Cultivation Project of Henan University (2019YLZDYJ02).

References

1 Q. Y. Li, L. Zhang, J. L. Dai, H. Tang, Q. Li, H. G. Xue and H. Pang, *Chem. Eng. J.*, 2018, **351**, 441–461.
2 J. J. Berzelius, *Pogg. Ann.*, 1826, **82**, 369–392.
3 J. F. Keggin, *Proc. R. Soc. London, Ser. A*, 1934, **144**, 75–100.
4 J.-W. Zhao, Y.-Z. Li, L.-J. Chen and G.-Y. Yang, *Chem. Commun.*, 2016, **52**, 4418–4445.
5 X. L. Chen, Y. Zhou, V. A. L. Roy and S.-T. Han, *Adv. Mater.*, 2018, **30**, 1703950.
6 A. Bijelic, M. Aureliano and A. Rompel, *Angew. Chem., Int. Ed.*, 2019, **58**, 2980–2999.
7 Y.-J. Liu, M.-T. Jin, L.-J. Chen and J.-W. Zhao, *Acta Crystallogr., Sect. C: Struct. Chem.*, 2018, **74**, 1202–1221.
8 J.-X. Liu, N. V. Izarova and P. Kögerler, *Chem. Commun.*, 2019, **55**, 10744–10747.
9 D. D. Li, P. T. Ma, J. Y. Niu and J. P. Wang, *Coord. Chem. Rev.*, 2019, **392**, 49–80.
10 X. Ma, H. L. Li, L. J. Chen and J. W. Zhao, *Dalton Trans.*, 2016, **45**, 4935–4960.
11 C. Boskovic, *Acc. Chem. Res.*, 2017, **50**, 2205–2214.
12 U. Warzok, L. K. Mahnke and W. Bensch, *Chem. – Eur. J.*, 2019, **25**, 1405–1419.
13 J. C. Liu, Q. Han, L. J. Chen and J. W. Zhao, *CrystEngComm*, 2016, **18**, 842–862.
14 M. Stuckart and K. Y. Monakhov, *Chem. Sci.*, 2019, **10**, 4364–4376.
15 X.-X. Li, D. Zhao and S.-T. Zheng, *Coord. Chem. Rev.*, 2019, **397**, 220–240.
16 L. Vilà-Nadal and L. Cronin, *Nat. Rev. Mater.*, 2017, **2**, 17054.
17 W. Jiang, X.-M. Liu, J. Liu, J. Shia, J.-P. Cao, X.-M. Luo, W.-S. You and Y. Xu, *Chem. Commun.*, 2019, **55**, 9299–9302.
18 M. Ibrahim, V. Mereacre, N. Leblanc, W. Wernsdorfer, C. E. Anson and A. K. Powell, *Angew. Chem., Int. Ed.*, 2015, **54**, 15574–15578.
19 J. C. Liu, J. Luo, Q. Han, J. Cao, L. J. Chen, Y. Song and J. W. Zhao, *J. Mater. Chem. C*, 2017, **5**, 2043–2055.
20 H. Wang, S. Hamanaka, Y. Nishimoto, S. Irle, T. Yokoyama, H. Yoshikawa and K. Awaga, *J. Am. Chem. Soc.*, 2012, **134**, 4918–4924.
21 S.-S. Wang and G.-Y. Yang, *Chem. Rev.*, 2015, **115**, 4893–4962.
22 R. Naseer, S. S. Mal, U. Kortz, G. Armstrong, F. Laffir, C. Dickinson, M. Vagin and T. McCormac, *Electrochim. Acta*, 2015, **176**, 1248–1255.
23 H.-Y. Zang, J.-J. Chen, D.-L. Long, L. Cronin and H. N. Miras, *Adv. Mater.*, 2013, **25**, 6245–6249.
24 W. M. Xuan, R. Pow, D.-L. Long and L. Cronin, *Angew. Chem., Int. Ed.*, 2017, **56**, 9727–9731.
25 Q. Zheng, L. Vilà-Nadal, Z. L. Lang, J.-J. Chen, D.-L. Long, J. S. Mathieson, J. M. Poblet and L. Cronin, *J. Am. Chem. Soc.*, 2018, **140**, 2595–2601.
26 Z. Li, L. L.-D. Lin, H. Yu, X.-X. Li and S.-T. Zheng, *Angew. Chem., Int. Ed.*, 2018, **57**, 15777–15781.
27 Q. Gao, X.-L. Wang, J. Xu and X.-H. Bu, *Chem. – Eur. J.*, 2016, **22**, 9082–9086.
28 X.-B. Han, Y.-G. Li, Z.-M. Zhang, H.-Q. Tan, Y. Lu and E.-B. Wang, *J. Am. Chem. Soc.*, 2015, **137**, 5486–5493.
29 L. Huang, S.-S. Wang, J.-W. Zhao, L. Cheng and G.-Y. Yang, *J. Am. Chem. Soc.*, 2014, **136**, 7637–7642.
30 S.-T. Zheng, J. Zhang, X.-X. Li, W.-H. Fang and G.-Y. Yang, *J. Am. Chem. Soc.*, 2010, **132**, 15102–15103.
31 L. Jin, X.-X. Li, Y.-J. Qi, P.-P. Niu and S.-T. Zheng, *Angew. Chem., Int. Ed.*, 2016, **55**, 13793–13797.
32 Y. J. Liu, H. L. Li, C. T. Lu, P. J. Gong, X. Y. Ma, L. J. Chen and J. W. Zhao, *Cryst. Growth Des.*, 2017, **17**, 3917–3928.

33 J.-C. Liu, Q. Han, L.-J. Chen, J.-W. Zhao, C. Streb and Y.-F. Song, *Angew. Chem., Int. Ed.*, 2018, **57**, 8416–8420.

34 Q. Han, Z. Li, X. M. Liang, Y. Ding and S.-T. Zheng, *Inorg. Chem.*, 2019, **58**, 12534–12537.

35 Z. Li, X.-X. Li, T. Yang, Z.-W. Cai and S.-T. Zheng, *Angew. Chem., Int. Ed.*, 2017, **56**, 2664–2669.

36 S. Reinoso, M. Giménez-Marqués, J. R. Galán-Mascarós, P. Vitoria and J. M. Gutiérrez-Zorrilla, *Angew. Chem., Int. Ed.*, 2010, **49**, 8384–8388.

37 M. H. Rosnes, C. Musumeci, C. P. Pradeep, J. S. Mathieson, D.-L. Long, Y.-F. Song, B. Pignataro, R. Cogdell and L. Cronin, *J. Am. Chem. Soc.*, 2010, **132**, 15490–15492.

38 C. Dey, T. Kundu and R. Banerjee, *Chem. Commun.*, 2012, **48**, 266–268.

39 Y. Wang, X. P. Sun, S. Z. Li, P. T. Ma, J. Y. Niu and J. P. Wang, *Cryst. Growth Des.*, 2015, **15**, 2057–2063.

40 Q. Han, J.-C. Liu, Y. Wen, L.-J. Chen, J.-W. Zhao and G.-Y. Yang, *Inorg. Chem.*, 2017, **56**, 7257–7269.

41 W. Salomon, G. Paille, M. Gomez-Mingot, P. Mialane, J. Marrot, C. Roch-Marchal, G. Nocton, C. Mellot-Draznieks, M. Fontecave and A. Dolbecq, *Cryst. Growth Des.*, 2017, **17**, 1600–1609.

42 Y.-F. Song and R. Tsunashima, *Chem. Soc. Rev.*, 2012, **41**, 7384–7402.

43 T. J. Greenfield, M. Julve and R. P. Doyle, *Coord. Chem. Rev.*, 2019, **384**, 37–64.

44 M. Natali, F. Nastasi, F. Puntoriero and A. Sartorel, *Eur. J. Inorg. Chem.*, 2019, 2027–2039.

45 R. Celiesiute, A. Ramanaviciene, M. Gicevicius and A. Ramanavicius, *Crit. Rev. Anal. Chem.*, 2019, **49**, 195–208.

46 C.-G. Lin, J. Hu and Y.-F. Song, *Adv. Inorg. Chem.*, 2017, **69**, 181–212.

47 L. Chen, W.-L. Chen, X.-L. Wang, Y.-G. Li, Z.-M. Su and E.-B. Wang, *Chem. Soc. Rev.*, 2019, **48**, 260–284.

48 Y. T. Zhang, H. M. Gan, C. Qin, X. L. Wang, Z. M. Su and M. J. Zaworotko, *J. Am. Chem. Soc.*, 2018, **140**, 17365–17368.

49 S. D. Adhikary, A. Tiwari, T. C. Nagaiah and D. Mandal, *ACS Appl. Mater. Interfaces*, 2018, **10**, 38872–38879.

50 F. M. Santos, P. Brandão, V. Félix, M. R. M. Domingues, J. S. Amaral, V. S. Amaral, H. I. S. Nogueiraa and A. M. V. Cavaleiro, *Dalton Trans.*, 2012, **41**, 12145–12155.

51 P. L. He, B. Xu, X. B. Xu, L. Song and X. Wang, *Chem. Sci.*, 2016, **7**, 1011–1015.

52 A. Klaiber and S. Polarz, *ACS Nano*, 2016, **10**, 10041–10048.

53 S. Landsmann, C. Lizandara-Pueyo and S. Polarz, *J. Am. Chem. Soc.*, 2010, **132**, 5315–5321.

54 J. J. Giner-Casares, G. Brezesinski, H. Möhwald, S. Landsmann and S. Polarz, *J. Phys. Chem. Lett.*, 2012, **3**, 322–326.

55 S. Landsmann, M. Luka and S. Polarz, *Nat. Commun.*, 2012, **3**, 1299.

56 S. Landsmann, M. Wessig, M. Schmid, H. Cölfen and S. Polarz, *Angew. Chem., Int. Ed.*, 2012, **51**, 5995–5999.

57 A. Klaiber, S. Landsmann, T. Löfflera and S. Polarz, *New J. Chem.*, 2016, **40**, 919–922.

58 S. Sutter, B. Trepka, S. Siroky, K. Hagedorn, S. Theiß, P. Baum and S. Polarz, *ACS Appl. Mater. Interfaces*, 2019, **11**, 15936–15944.

59 P. J. Barczuk, A. Lewera, K. Miecznikowski, A. Zurowski and P. J. Kulesza, *J. Power Sources*, 2010, **195**, 2507–2513.

60 S.-X. Guo, F. W. Li, L. Chen, D. R. MacFarlane and J. Zhang, *ACS Appl. Mater. Interfaces*, 2018, **10**, 12690–12697.

61 S. S. Hassan, Y. P. Liu, Sirajuddin, A. R. Solangi, A. M. Bond and J. Zhang, *Anal. Chim. Acta*, 2013, **803**, 41–46.

62 H. Taghiyar and B. Yadollahi, *Sci. Total Environ.*, 2019, 134860.

63 X.-J. Feng, W. Yao, M.-F. Luo, R.-Y. Ma, H.-W. Xie, Y. Yu, Y. G. Li and E.-B. Wang, *Inorg. Chim. Acta*, 2011, **368**, 29–36.

64 J. Y. Han, D. P. Wang, Y. H. Du, S. B. Xi, Z. Chen, S. M. Yin, T. H. Zhou and R. Xu, *Appl. Catal., A*, 2016, **521**, 83–89.

65 D. M. Fernandes, A. D. S. Barbosa, J. Pires, S. S. Balula, L. Cunha-Silva and C. Freire, *ACS Appl. Mater. Interfaces*, 2013, **5**, 13382–13390.

66 S. Mukhopadhyay, J. Debgupta, C. Singh, A. Kar and S. K. Das, *Angew. Chem.*, 2018, **130**, 1936–1941.

67 R. Li, X. Q. Ren, J. S. Zhao, X. Feng, X. Jiang, X. X. Fan, Z. G. Lin, X. G. Li, C. W. Hu and B. Wang, *J. Mater. Chem. A*, 2014, **2**, 2168–2173.

68 R. J. Liu, G. J. Zhang, H. B. Cao, S. J. Zhang, Y. B. Xie, A. Haider, U. Kortz, B. H. Chen, N. S. Dalal, Y. S. Zhao, L. J. Zhi, C.-X. Wu, L.-K. Yan, Z. M. Su and B. Keita, *Energy Environ. Sci.*, 2016, **9**, 1012–1023.

69 W. H. Guo, X. L. Tong and S. B. Liu, *Electrochim. Acta*, 2015, **173**, 540–550.

70 D. M. Fernandes and C. Freire, *ChemElectroChem*, 2015, **2**, 269–279.

71 D. M. Fernandes, M. P. Araújo, A. Haider, A. S. Mougharbel, A. J. S. Fernandes, U. Kortz and C. Freire, *ChemElectroChem*, 2018, **5**, 273–283.

72 A. K. Cuentas-Gallegos, M. Miranda-Hernández and A. Vargas-Ocampo, *Electrochim. Acta*, 2009, **54**, 4378–4383.

73 X. X. Zhang, Y. Y. Bao, Y. F. Bai, Z. Z. Chen, J. Li and F. Feng, *Electrochim. Acta*, 2019, **300**, 380–388.

74 F. Boussema, A. J. Gross, F. Hmida, B. Ayed, H. Majdoub, S. Cosnier, A. Maaref and M. Holzinger, *Biosens. Bioelectron.*, 2018, **109**, 20–26.

75 R. Naseer, S. S. Mal, M. Ibrahim, U. Kortz, G. Armstrong, F. Laffir, C. Dickinson, M. Vagin and T. McCormac, *Electrochim. Acta*, 2014, **134**, 450–458.

76 N. Anwar, A. Sartorel, M. Yaqub, K. Wearen, F. Laffir, G. Armstrong, C. Dickinson, M. Bonchio and T. McCormac, *ACS Appl. Mater. Interfaces*, 2014, **6**, 8022–8031.

77 M. Blasco-Ahicart, J. Soriano-López and J. R. Galán-Mascarós, *ChemElectroChem*, 2017, **4**, 3296–3301.

78 D. W. Fan, X. F. Jia, P. Q. Tang, J. C. Hao and T. B. Liu, *Angew. Chem., Int. Ed.*, 2007, **46**, 3342–3345.
79 L. Zhang, L. Chen, S. X. Liu, J. Gong, Q. Tang and Z.-M. Su, *Dalton Trans.*, 2018, **47**, 105–111.
80 S. Zoladek, I. A. Rutkowsk and P. J. Kulesza, *Appl. Surf. Sci.*, 2011, **257**, 8205–8210.
81 S.-M. Liu, Z. Zhang, X. H. Li, H. J. Jia, M. W. Ren and S. X. Liu, *Adv. Mater. Interfaces*, 2018, **5**, 1801062.
82 R. J. Liu, S. W. Li, X. L. Yu, G. J. Zhang, Y. Ma and J. N. Yao, *J. Mater. Chem.*, 2011, **21**, 14917–14924.
83 R. J. Liu, S. W. Li, X. L. Yu, G. J. Zhang, S. J. Zhang, J. N. Yao, B. Keita, L. Nadjo and L. J. Zhi, *Small*, 2012, **8**, 1398–1406.
84 R. J. Liu, X. L. Yu, G. J. Zhang, S. J. Zhang, H. B. Cao, A. Dolbecq, P. Mialane, B. Keita and L. J. Zhi, *J. Mater. Chem. A*, 2013, **1**, 11961–11969.
85 L. J. Hong, Y. H. Gui, J. Lu, J. G. Hu, J. H. Yuan and L. Niu, *Int. J. Hydrogen Energy*, 2013, **38**, 11074–11079.
86 A. Ma, X. F. Zhang, Z. S. Li, X. Y. Wang, L. T. Ye and S. Lin, *J. Electrochem. Soc.*, 2014, **161**, F1224–F1230.
87 L. Suo, W. M. Gao, Y. Du, R. Q. Wang, L. X. Wu and L. H. Bi, *New J. Chem.*, 2016, **40**, 985–993.
88 S. S. Zhang, R. J. Liu, S. W. Li, A. Dolbecq, P. Mialane, L. Suo, L. H. Bi, B. F. Zhang, T. B. Liu, C. X. Wu, L. K. Yan, Z. M. Su, G. J. Zhang and B. Keita, *J. Colloid Interface Sci.*, 2018, **514**, 507–516.
89 J. Liu, J. Wang, W.-B. Wang, M. Chen and D.-J. Qian, *Appl. Surf. Sci.*, 2017, **408**, 68–76.
90 R. M. Xing, L. Y. Tong, X. Y. Zhao, H. L. Liu, P. T. Ma, J. W. Zhao, X. Q. Liu and S. H. Liu, *Sens. Actuators, B*, 2019, **283**, 35–41.
91 B. P. Suma, P. S. Adarakatti, S. K. Kempahanumakkagari and P. Malingappa, *Mater. Chem. Phys.*, 2019, **229**, 269–278.
92 Y.-J. Tang, H.-J. Zhu, L.-Z. Dong, A.-M. Zhang, S.-L. Li, J. Liu and Y.-Q. Lan, *Appl. Catal., B*, 2019, **245**, 528–535.
93 T. Ueda, *ChemElectroChem*, 2018, **5**, 823–838.
94 O. Nakamura, T. Kodama, I. Ogino and Y. Miyake, *Chem. Lett.*, 1979, **8**, 17–18.
95 G.-J. Cao, J.-D. Liu, T.-T. Zhuang, X.-H. Cai and S.-T. Zheng, *Chem. Commun.*, 2015, **51**, 2048–2051.
96 Y.-Q. Jiao, H.-Y. Zang, X.-L. Wang, E.-L. Zhou, B.-Q. Song, C.-G. Wang, K.-Z. Shao and Z.-M. Su, *Chem. Commun.*, 2015, **51**, 11313–11316.
97 Y. W. Liu, X. Yang, J. Miao, Q. Tang, S. M. Liu, Z. Shi and S. X. Liu, *Chem. Commun.*, 2014, **50**, 10023–10026.
98 Y. W. Liu, S. M. Liu, X. Y. Lai, J. Miao, D. F. He, N. Li, F. Luo, Z. Shi and S. X. Liu, *Adv. Funct. Mater.*, 2015, **25**, 4480–4485.
99 T. Iwano, S. Miyazawa, R. Osuga, J. N. Kondo, K. Honjo, T. Kitao, T. Uemura and S. Uchida, *Commun. Chem.*, 2019, **2**, 9.
100 G. L. Cao, J. Xiong, Q. Xue, S. T. Min, H. M. Hu and G. L. Xue, *Electrochim. Acta*, 2013, **106**, 465–471.
101 G. Rousseau, S. S. Zhang, O. Oms, A. Dolbecq, J. Marrot, R. J. Liu, X. K. Shang, G. J. Zhang, B. Keita and P. Mialane, *Chem. – Eur. J.*, 2015, **21**, 12153–12160.
102 R. Wan, H. F. Li, X. Y. Ma, Z. Liu, V. Singh, P. T. Ma, C. Zhang, J. Y. Niu and J. P. Wang, *Dalton Trans.*, 2019, **48**, 10327–10336.
103 Y.-R. Wang, Q. Huang, C.-T. He, Y. F. Chen, J. Liu, F.-C. Shen and Y.-Q. Lan, *Nat. Commun.*, 2018, **9**, 4466.
104 C. Singh, S. Mukhopadhyay and S. K. Das, *Inorg. Chem.*, 2018, **57**, 6479–6490.
105 S. Imar, M. Yaqub, C. Maccato, C. Dickinson, F. Laffir, M. Vagin and T. McCormac, *Electrochim. Acta*, 2015, **184**, 323–330.
106 O. Oms, S. Yang, W. Salomon, J. Marrot, A. Dolbecq, E. Riviere, A. Bonnefont, L. Ruhlmann and P. Mialane, *Inorg. Chem.*, 2016, **55**, 1551–1561.
107 W. J. Luo, J. Hu, H. L. Diao, B. Schwarz, C. Streb and Y.-F. Song, *Angew. Chem., Int. Ed.*, 2017, **56**, 4941–4944.
108 X. L. Wang, J. J. Sun, H. Y. Lin, Z. H. Chang, G. C. Liu and X. Wang, *CrystEngComm*, 2017, **19**, 3167–3177.
109 H. Y. Ma, Z. J. Zhang, H. J. Pang, S. Li, Y. Y. Chen and W. J. Zhang, *Electrochim. Acta*, 2012, **69**, 379–383.
110 F. Boussema, R. Haddad, Y. Ghandour, M. S. Belkhiria, M. Holzinger, A. Maaref and S. Cosnier, *Electrochim. Acta*, 2016, **222**, 402–408.
111 M. García, K. Carfumán, C. Díaz, C. Garrido, I. Osorio-Román, M. J. Aguirre and M. Isaacs, *Electrochim. Acta*, 2012, **80**, 390–398.
112 Y. F. Zhang, X. J. Bo, A. Nsabimana, A. Munyentwali, C. Han, M. Li and L. P. Guo, *Biosens. Bioelectron.*, 2015, **66**, 191–197.
113 L. Kang, H. Y. Ma, Y. Yu, H. J. Pang, Y. B. Song and D. Zhang, *Sens. Actuators, B*, 2013, **177**, 270–278.
114 Q. Gao, D.-H. Hu, D. H. Li, M.-H. Duan and Y. Wu, *Inorg. Chim. Acta*, 2019, **487**, 107–111.
115 Z. J. Fu, W. M. Gao, T. Yu and L. H. Bi, *Talanta*, 2019, **195**, 463–471.
116 C. L. Zhou, S. Li, W. Zhu, H. J. Pang and H. Y. Ma, *Electrochim. Acta*, 2013, **113**, 454–463.
117 L. H. Zhang, Q. W. Wang, Y. Qi, L. Li, S. T. Wang and X. H. Wang, *Sens. Actuators, B*, 2019, **288**, 347–355.
118 Y. M. Li, H. L. Li, J. Jiang, L. J. Chen and J. W. Zhao, *Inorg. Chem.*, 2019, **58**, 3479–3491.